

Procedure for Predicting Lower Critical Solution Temperature Behavior in Binary Blends of Polymers

P. A. Rodgers, D. R. Paul, and J. W. Barlow*

Department of Chemical Engineering and Center for Polymer Research, The University of Texas at Austin, Austin, Texas 78712

Received October 5, 1990; Revised Manuscript Received February 18, 1991

ABSTRACT: A procedure is presented that uses heat of mixing information, calculated by the modified Guggenheim quasichemical (MGQ) group contribution method, and PVT data for the polymers, correlated by the Sanchez-Lacombe-Balasz (SLB) lattice fluid model, to predict lower critical solution temperature (LCST) behavior. Fairly good predictions, to within 20 °C uncertainty, of cloud points are shown for poly(vinyl methyl ether)/poly(styrene) (PVME/PS), poly(methyl methacrylate)/poly(vinyl chloride) (PMMA/PVC), and poly(methyl methacrylate)/poly(ethylene oxide) (PMMA/PEO) binary blends.

Introduction

The formation of miscible polymer blends, blends that are homogeneous at the polymer segment level of scale, is well-known to require that the free energy of mixing, ΔG_{mix} , be negative.¹⁻⁶ In addition, the formation of a totally miscible system also requires

$$(\partial^2 \Delta G_{\text{mix}} / \partial \phi_i^2)_{T,P} > 0 \quad (1)$$

to ensure stability against phase separation, where ϕ_i is the volume fraction of component i , T the absolute temperature, and P the pressure. The free energy of mixing has both enthalpic (ΔH_{mix}) and entropic (ΔS_{mix}) contributions

$$\Delta G_{\text{mix}} = \Delta H_{\text{mix}} - T\Delta S_{\text{mix}} \quad (2)$$

and these contributions are generally functions of composition, temperature, and, in the case of ΔS_{mix} , molecular weight. The entropic contribution is quite small at the molecular weights normally encountered in commercial polymers, however, and the requirement that $\Delta G_{\text{mix}} < 0$ is equivalent to requiring the heat of mixing to be exothermic or negative.

Considerable progress toward finding new miscible polymer ternaries⁷ and binaries⁸⁻¹⁵ has been made, in part, by recognizing the importance of exothermic physical enthalpic interactions for determining phase behavior. The heat of mixing between polymer segments is found, experimentally,⁷⁻¹⁵ to be nearly equivalent to the heat of mixing of low molecular weight compounds that have structures that are similar to those of the segments. This result, which is expected from various statistical mechanical formulations of the liquid state¹⁶⁻²¹ by the assumption that enthalpic interactions are primarily a function of nearest neighbor functional groups, permits the use of exothermic heats of mixing of low molecular weight compounds to indicate probable miscibility of the corresponding polymer binaries.

The success of the analogue heats of mixing approach for suggesting miscibility of polymers has stimulated the application of the modified Guggenheim quasichemical (MGQ) group contribution method, based on heats of mixing data for liquids, for predicting polymer blend miscibility.²²⁻²⁴ As the name implies, the MGQ method is based on an empirical modification of the Guggenheim quasichemical theory.^{16,21,22} This method is used only to correlate and calculate the heat of mixing function in terms of group contributions and seems to do a good job of predicting interactions between polar and nonpolar liquids

at different temperatures and compositions.²² The calculated heat of mixing is found to be sufficient to predict the "window of miscibility" within which aliphatic polyesters with varying carbonyl to CH_2 ratios in their segment structures are found to be miscible with poly(vinyl chloride) (PVC), polycarbonate, tetramethylpolycarbonate, and Phenoxy, the polyhydroxy ether of Bisphenol A.^{22,23} Within the window, heats of mixing of the polymers are predicted to be exothermic, indicating that miscible blend formation is possible, and miscible blends are found experimentally. Outside the window, calculated heats of mixing are endothermic, and the blends are experimentally found to be immiscible.

When sufficiently heated, mixtures of low molecular weight liquids that show exothermic heats of mixing often transition from single-phase, miscible, behavior to multiphase behavior.²⁰ This transition, called the lower critical solution temperature (LCST), is also often seen in miscible polymer blends.²⁵⁻³² The LCST transition is thought to occur when the stability criterion, eq 1, or its equivalent,

$$\left(\frac{\partial^2 G}{\partial \phi^2} \right)_V + \left(\frac{\partial V}{\partial P} \right)_{T,\phi} \left(\frac{\partial^2 G}{\partial \phi_i \partial V} \right)^2 > 0 \quad (3)$$

where G is the free energy, V the volume, and P the pressure, is violated. Equation 3 becomes negative when the system becomes unstable. The term, $\partial V / \partial P$, is related to the system compressibility and is a function of the equation of state for the mixture. This so-called "equation of state" contribution to the stability criterion is always negative, and systems tend to become more compressible with increasing temperature. Consequently, the finite compressibility of the mixture provides a mechanism for LCST behavior.

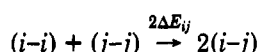
Equation 3 suggests that phase stability occurs when the first term dominates and is positive. This term is positive when the curve of G vs ϕ_i , the free energy "well", is concave up, and the magnitude of this term is proportional to the depth of the well. From the arguments above, the depth of the well is directly related to the magnitude of the exothermic heat of mixing for mixtures of high molecular weight materials. The heat of mixing of any system tends toward zero as the temperature of the system is raised and the mixture approaches the thermodynamic ideal limit. Consequently, raising the temperature of the mixture can, in principle, reduce the magnitude of the first term in eq 3 sufficiently to allow domination by the second term and resulting phase instability. This approach suggests that the temperature dependency of the heat of

mixing is potentially responsible for LCST behavior. Miscible polymer blends can show positive excess heat capacities, $C_p^E = \partial \Delta H_{\text{mix}}' / \partial T$, and hence can show reduced exothermic heats of mixing with increasing temperature.^{33,34} Crude correlations between the magnitude of the exothermic heat of mixing at the melting point of one of the blend components and the cloud temperature also suggest that the LCST occurs at a temperature where the first term in eq 3 has been sufficiently reduced.¹⁵

This paper combines the heats of mixing prediction of the MGQ method with the generalized lattice fluid equation of state SLB model, by Sanchez-Lacombe-Balasz,^{35,36} to predict the LCST behavior by use of the general stability criterion, eq 3. In this approach, the MGQ group contribution method is used to estimate the heat of mixing as a function of composition and temperature. The parameters for this method, discussed below, are obtained from heats of mixing data for liquids containing the same groups as those in the polymer segments. PVT data for the polymers are analyzed by the SLB model to obtain the pure component parameters required for estimating the mixture properties by this model. Two unknown, energy-related, parameters in the SLB model are evaluated by requiring that the predicted heat of mixing by the model equal that predicted by the MGQ model. This requirement then permits the prediction of the LCST, via eq 3, without the need for adjustable parameters. The important features of these models and their use are summarized below.

Thermodynamic Models

Modified Guggenheim Quasichemical (MGQ) Model. The MGQ model²²⁻²⁴ is based on a quasichemical model, proposed by Guggenheim,¹⁸ for predicting changes in thermodynamic properties associated with the mixing of liquids. The MGQ model considers the heat of mixing to arise from the energies associated with the formation of i - j from the i - i and j - j contacts identified with the pure components i and j



$$\frac{N_{ij}^2}{N_{ii}N_{jj}} = K_{ij} = A_{ij} \exp(-2\Delta E_{ij}/RT) \quad (4)$$

where N_{ij} is the moles of i - j contact pairs and ΔE_{ij} is the energy change associated with the formation of an i - j pair. The addition of the parameter A_{ij} to Guggenheim's original theory is an empirical modification that greatly improves the ability of the model to fit and to predict heats of mixing.²² The rationale for including it involves considering K_{ij} to be a "true" chemical equilibrium constant, from which it follows that A_{ij} is related to the exchange entropy, ΔS_{ij} , via

$$A_{ij} = \exp(2\Delta S_{ij}/RT) \quad (5)$$

The number of equilibrium contact pairs, N_{ij} , can be related to the number of structural groups, n_i and n_j , through a series of standard relationships.^{18,19,21,37} Each group is considered to have zq_i nearest neighbors, where $z = 10$ is the standard coordination number, and where q_i is a parameter that is proportional to its surface area, A_{wi} , as defined by Bondi³⁷

$$q_i = A_{wi}/(2.5 \times 10^9) \quad (6)$$

The average area fraction of n_i groups is then

$$\Psi_i = q_i n_i / A_t \quad (7)$$

where

$$A_t = \sum_i q_i n_i \quad (8)$$

The number of contacts for the locally nonrandom, nonathermal, mixture is then given by

$$N_{ij} = N_{ji} = \Gamma_{ij} z A_t \Psi_i \Psi_j \quad N_{ii} = \Gamma_{ii} (z/2) A_t \Psi_i^2 \quad (9a)$$

where Γ is the nonrandom parameter²¹ that expresses the deviations in local composition from the global average. This parameter is symmetric ($\Gamma_{ij} = \Gamma_{ji}$), and the conservation of contact sites further requires that

$$\sum_j \Psi_j \Gamma_{ji} = 1 \quad (9b)$$

The nonrandom parameter can be evaluated for each i - j pair by combining eqs 10, 9a,b, and 4

$$\frac{\Gamma_{ij}^2 \Psi_i \Psi_j}{(1 - \sum_{j \neq i} \Psi_j \Gamma_{ij})(1 - \sum_{i \neq j} \Psi_i \Gamma_{ij})} = K_{ij} \quad (10)$$

In a system containing f different functional groups, calculation of the Γ_{ij} parameters requires the simultaneous solution of $f(f-1)/2$ equations, each of the form of eq 10.

The heat of mixing of groups is then²²

$$\Delta H_{\text{mix}} \approx \Delta U_{\text{mix}} = z A_t \sum_i \sum_{j>i} \Gamma_{ij} \Delta E_{ij} \Psi_i \Psi_j \quad (11)$$

The heat of mixing of two real fluids must account for the "self-interactions" that occur between the structural groups that comprise the pure component molecules to be mixed. This can be accomplished by treating each pure component as if it were a separate solution of structural groups, and by subtracting the "heats of mixing" associated with the pure component "solutions" of groups from that associated with the mixture of components.¹¹ This approach leads to a heat of mixing for the real multigroup fluids of the form

$$\Delta H_{\text{mix}}' = \Delta H_{\text{mix}} / V = \sum_i \sum_{j>i} B_{ij}' \Psi_i \Psi_j - \sum_k \sum_i \sum_{j>i} \Phi_k B_{ij}'^{(k)} \Psi_i^{(k)} \Psi_j^{(k)} \quad (12)$$

where Φ_k is the volume fraction of pure component k in the solution, $\Psi_j^{(k)}$ is the area fraction of group j in pure component k , and B_{ij}' is the interaction energy density for the i - j interaction

$$B_{ij}' = (A_t/V) \Gamma_{ij} \Delta E_{ij} \quad (13)$$

and $B_{ij}'^{(k)}$ is evaluated for the "solution" of groups for each pure component k by application of the method, outlined above, at the same temperature.

Equation 12 is identical in form with the binary interaction model for copolymers, proposed earlier.¹¹ In the present formulation, however, the interaction parameters B_{ij}' are functions of both temperature and composition, through eq 4. As expected from the formulation above, K_{ij} , Γ_{ij} , B_{ij}' , and ΔH_{mix} approach zero as the temperature is increased. While the temperature dependency of the heat of mixing for polymers is generally not known, the MGQ model appears to be able to correctly estimate the temperature dependency of the heat of mixing for mixtures of alcohols with alkanes, where hydrogen bonding is important.²² To the extent that the heat of mixing of polymer segments is identical with that of small molecules made of the same structural groups, the MGQ model may give a reasonable estimate of the heats of mixing for polymer binaries at high temperatures where LCST behavior is likely to occur.

SLB Lattice Fluid Model. The detailed development and application of the SLB lattice fluid model is presented

elsewhere^{35,36} and only the equations pertinent to the present work are discussed here. At zero pressure, the free energy per mer, g , of a binary mixture of N_1 molecules, which occupy r_1 lattice sites, with N_2 molecules of size r_2 is given by

$$g = -\rho_r \epsilon_T^* - T(s_c + s_v) \quad (14)$$

where s_c is the Flory-Huggins entropy of mixing per mer associated with mixing of occupied lattice sites

$$-s_c/k = (\Phi_1/r_1) \ln(\Phi_1) + (\Phi_2/r_2) \ln(\Phi_2) \quad (15)$$

and s_v is the entropy of mixing of lattice sites with vacancies

$$-s_v/k = ((1 - \rho_r)/\rho_r) \ln(1 - \rho_r) + (1/r) \ln(\rho_r) \quad (16)$$

In eqs 14–16, the term ρ_r is the reduced density of the mixture and equals the fraction of occupied lattice sites, Φ_i is the volume fraction of component i at zero temperature ($\rho_r = 1$), as defined by

$$\Phi_i = r_i N_i / \sum_j r_j N_j \quad (17)$$

The size parameter, r_i , for each pure component is computed from the molecular weight, M , and from the characteristic, starred, parameters, via

$$r_i = M/(\rho_i^* \nu_{oi}) \quad (18)$$

where the parameter ν_{oi} is the characteristic volume per mole of sites, given by

$$\nu_{oi} = (RT_i^*)/P_i^* \quad (19)$$

The volume of the system is computed by

$$V = (r_1 N_1 + r_2 N_2) \nu_o / \rho_r \quad (20)$$

where the characteristic volume per mole of sites, ν_o , is given by

$$1/\nu_o = \Phi_1/\nu_{o1} + \Phi_2/\nu_{o2} \quad (21)$$

for the binary mixture.

The characteristic parameters, T_i^* , P_i^* , and ρ_i^* , are evaluated from PVT data for the pure components, using the high molecular weight form³⁵ of the reduced equation of state, which is associated with eq 14

$$\rho_r^2 + P_r + T_r [\ln(1 - \rho_r) + \rho_r] = 0 \quad (22)$$

where $\rho_r = \rho_i/\rho_i^*$, $P_r = P/P_i^*$, and $T_r = T/T_i^*$ are the reduced parameters representing density, pressure, and temperature, ρ_i , P , and T , respectively. The characteristic parameters can be determined by a nonlinear least-squares fit of eq 22 to the PVT data. This procedure yields a set of parameters that best fit the experimental densities over the pressure and temperature ranges considered. An alternative approach that is useful when data are limited first obtains the parameters ρ_i^* and T_i^* by setting $P_r = 0$ in eq 22 and fitting this approximation to atmospheric density vs temperature data. The characteristic pressure is then determined by comparing the theoretical reduced isothermal compressibility at zero pressure

$$\begin{aligned} \beta_{rio} &= (1/\rho_{ri})(\partial \rho_{ri} / \partial P_r)_{T_r, P_r=0} \\ &= (1/\rho_{ri})^2 (1 - \rho_{ri}) / (T_r - 2(1 - \rho_{ri})) \end{aligned} \quad (23)$$

with the experimental isothermal compressibility obtained by fitting the well-known Tait equation to the data

$$\begin{aligned} v &= 1/\rho_i = A(T) \{1 - 0.0894 \ln[1 + P/B(T)]\} \\ \beta_{io} &= -(1/v)(\partial v / \partial P)_{T, P=0} = 0.0894/B(T) \end{aligned} \quad (24)$$

where $B(T)$ is the Tait parameter, which is usually fit to the form $B(T) = B_o \exp(-B_1 T)$. The characteristic parameter, $P^* = \beta_{rio}/\beta_{io}$, is typically evaluated at several points over the range of experimental temperature where compressibility data are available. Values of P^* are found to increase slightly with increasing temperature and are either averaged or fit to a polynomial in temperature to describe the variation.

The enthalpy parameter, ϵ_T^* , for the mixture, eq 14, is a function of temperature and composition

$$\epsilon_T^* = \Phi_1^2 \epsilon_1^* + 2\Phi_1 \Phi_2 g_{12}^* + \Phi_2^2 \epsilon_2^* \quad (25)$$

where ϵ_i^* is the characteristic energy of interaction for component i , a value that is related to the characteristic temperature, T_i^* , via

$$\epsilon_i^* = k T_i^* \quad (26)$$

The parameter, g_{12}^* , is a free energy parameter associated with the interaction of 1 with 2. In the Sanchez-Balazs³⁶ modification of the Sanchez-LaCombe³⁵ model, which we are calling the SLB model, the parameter is defined as

$$g_{12}^* = \epsilon_{12}^* + \delta \epsilon^* - RT \ln[(1 + d)D] \quad (27)$$

$$D = (1 + d \exp(-\delta \epsilon^*/kT))^{-1} \quad (28)$$

The energy parameter ϵ_{12}^* is that associated with non-specific interactions, assumed to be temperature independent, and $\delta \epsilon^*$ is the additional energy associated with the strong specific interaction, which is temperature dependent. The parameter d is a statistical degeneracy related to the number of ways the specific 1–2 interaction can occur. It is assigned a value of 10 on the recommendation of Sanchez.³⁶ The parameters ϵ_{12}^* and $\delta \epsilon^*$ are generally not known from the properties of the pure components, although they have been evaluated by application of the SLB model to known PVT and LCST experimental data.³⁶

In this paper, we will use the MGQ model to estimate the heat of mixing from which ϵ_{12}^* and $\delta \epsilon^*$ can be obtained. To do this, we need to determine the heat of mixing for the SLB model. The enthalpy per mer of the mixture can be computed from eq 14 by

$$h = g + Ts \quad (29)$$

The entropy per mer is just

$$s = -dg/dT = s_c + s_v + 2\rho_r \Phi_1 \Phi_2 (dg_{12}^*/dT) \quad (30)$$

where $-dg_{12}^*/dT$ is the entropic contribution to the system from the g_{12}^* free energy parameter

$$dg_{12}^*/dT = -k \{ \ln[(1 + d)D] - (1 - D)\delta \epsilon^*/kT \} \quad (31)$$

Combining eqs 14 and 29–31 yields

$$\begin{aligned} h &= -\rho_r [\Phi_1^2 \epsilon_1^* + \Phi_2^2 \epsilon_2^* + 2\Phi_1 \Phi_2 (g_{12}^* - T(dg_{12}^*/dT))] \\ &= -\rho_r [\Phi_1^2 \epsilon_1^* + \Phi_2^2 \epsilon_2^* + 2\Phi_1 \Phi_2 (\epsilon_{12}^* + D\delta \epsilon^*)] \end{aligned} \quad (32)$$

The heat of mixing is then given by

$$\begin{aligned} \Delta H_{\text{mix}} &= H_m - H_1 - H_2 \\ &= (r_1 N_1 + r_2 N_2) h - r_1 N_1 (-\rho_{r1} \epsilon_1^*) - r_2 N_2 (-\rho_{r2} \epsilon_2^*) \end{aligned} \quad (33)$$

which can be rewritten as

$$\Delta H_{\text{mix}} = (r_1 N_1 + r_2 N_2) [-\rho_r h + \Phi_1 \rho_{r1} \epsilon_1^* + \Phi_2 \rho_{r2} \epsilon_2^*] \quad (34)$$

The heat of mixing per unit volume for the SLB model is

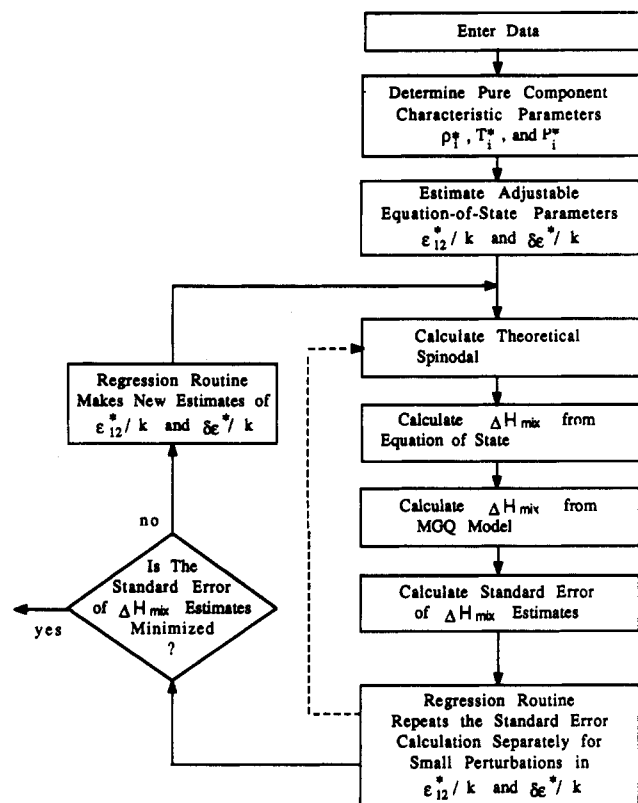


Figure 1. Calculational flow sheet for LCST prediction.

then computed from eqs 34 and 20 to be

$$\Delta H_{\text{mix}}/V = (\rho_r/\nu_o)[- \rho_r h + \Phi_1 \rho_{r1} \epsilon_1^* + \Phi_2 \rho_{r2} \epsilon_2^*] \quad (35)$$

The unknown mixing parameters ϵ_{12}^* and $\delta \epsilon^*$ can be evaluated from the pure component parameters, eq 35 and eq 12, by using the procedures discussed below.

The free energy of the binary system, G , can be written as

$$G = (r_1 N_1 + r_2 N_2)g \quad (36)$$

where g is defined by 14. Consequently, the criterion for phase stability, eq 3, becomes

$$\left(\frac{1}{r_1 \Phi_1} - \frac{1}{r_2 \Phi_2} \right) - \rho_r [-2\Delta \epsilon^*/kT + \Omega^2 T_r P^* \beta_o] > 0 \quad (37)$$

where

$$\Delta \epsilon^* = \epsilon_1^* + \epsilon_2^* - 2g_{12}^* \quad (38)$$

$$\Omega = \rho_r (d\epsilon_r^*/d\Phi_1)/kT - (1/r_1 - 1/r_2)$$

$$= (2\rho_r/kT)[\Phi_1 \epsilon_1^* + g_{12}^*(\Phi_2 - \Phi_1) + \Phi_2 \epsilon_2^*] - (1/r_1 - 1/r_2) \quad (39)$$

The first term on the left of eq 37 derives from the combinatorial entropy. The second term consists of two separate contributions; a term that contains $\Delta \epsilon^*$ and is derived from the heat of mixing, and a term that contains the compressibility and is related to free volume considerations.

Phase separation is primarily determined by the balancing of terms in eq 37. If the heat of mixing, hence $\Delta \epsilon^*$, is sufficiently positive, blends will show phase separation at low temperature. If $\Delta \epsilon^*$ is negative or nearly zero, then miscible solutions may be possible at low temperature, even though the system phase separates at higher temperature.

Calculational Procedure for Predicting LCST Behavior. Figure 1 shows a flow sheet of the FORTRAN

Table I
Equation of State Information Used in Calculations for the PS/PVME System

names of polymer components (up to four characters long)		PS	PVME
molecular weight of repeat unit	M_u	104.1	58.1
weight-average molecular weight	M_w	230 000	389 000
coefficients of specific volume vs temperature polynomial	a	0.9200	0.9335
$v = a + bt + ct^2 + dt^3$	b	5.102×10^{-4}	5.837×10^{-4}
(t in $^{\circ}\text{C}$, v in cm^3/g)	c	2.354×10^{-7}	1.034×10^{-7}
	d	0	0
coefficients of the Tait	B_0	2435.0	1885.1
parameter $B_{\text{Tait}} = B_0$	B_1	4.14×10^{-3}	6.20×10^{-3}
$\exp(-B_1 t)$ (t in $^{\circ}\text{C}$, B in bar)	v^*	0.8403	0.9091
characteristic equation of state	T^*	735.0	657.0
parameters (v^* in cm^3/g , T^*	P^*	85.5	86.7
in K, P^* in cal/cm^3)			

Table II
Structural Group Assignments and Characteristics for the PS/PVME System

structural group	MW/ q	type no.	class no.	no. of groups in PS	no. of groups in PVME
$>\text{CH}_2$	14.03/0.540	1	1	1	1
$>\text{CH}$	13.02/0.228	2	1	1	1
$=\text{CH- arom}$	13.02/0.400	3	2	5	0
$=\text{C}-\text{ arom}$	12.01/0.120	4	2	1	0
OCH_3	31.03/1.088	5	3	0	1

calculations used to predict LCST behavior from the models described above. In this program, called Polyphase, the unknown parameters are considered to be ϵ_{12}^*/k and $\delta \epsilon^*/k$. The program initially estimates ϵ_{12}^*/k and $\delta \epsilon^*/k$ to be small and negative. It then calculates the theoretical spinodal (temperature vs phase composition diagram) by application of eqs 27–39, over the entire composition range in increments of 0.05% by volume. The heat of mixing per unit volume at each spinodal temperature and composition is then calculated from eq 35. The heat of mixing per unit volume is also computed from the MGQ model at each spinodal temperature and composition, using eq 12. The root-mean-square error relative to the MGQ estimation is then computed for all the points comprising the spinodal and saved. New estimates of the parameters ϵ_{12}^*/k and $\delta \epsilon^*/k$ are then made and the process is repeated to yield a new error relative to the MGQ model. This error is compared with the previous value to obtain new estimates of the parameters. The process is repeated until the relative error is minimized to yield the “best” estimates of ϵ_{12}^* , $\delta \epsilon^*$, and the spinodal.

Summary of Input Data

PVME/PS. Typical input data for Polyphase are illustrated in Tables I–III for the PVME/PS system. All of the information is obtained from the experimental work of others. The polymer molecular weights are taken from data set 1 in the work of Han et al.²⁹ These data show experimental phase separation as determined by small-angle neutron scattering and are compared against the model predictions, below. The polynomial coefficients that describe the thermal dilatation of PS are determined from Richardson and Saville,³⁸ and those that describe the thermal behavior of poly(vinyl methyl ether) (PVME) are calculated from a density vs temperature polynomial in Uriarte et al.³⁹ The Tait parameters for PVME are fit from equations for thermal pressure and thermal expansion in ref 39, while those for poly(styrene) (PS) are fit from the data in ref 40. The characteristic parameters, v^* , P^* , and T^* , in Table I, were calculated from the thermal

Table III
MGQ Group Interaction and Entropy Parameters

structural groups ^a		systems studied	data pts	sources	A_{ij}	ΔE_{ij} , cal/mol	% rms error
<i>i</i>	<i>j</i>						
>CH ₂	=CH-arom	5	91	47-50	0.935	28.8	6
>CH ₂	OCH ₃	3	27	41	1.038	76.5	3
>CH ₂	CH ₂ COO	9	123	51-53	1.000	137.4	10
>CH ₂	CH ₂ O	5	46	41, 54	0.612	70.3	14
>CH ₂	>CHCl	3	23	22	0.438	78.3	4
=CH-arom	OCH ₃	3	13	42	1.087	0.985	6
CH ₂ O	CH ₂ COO	1	8	55	0.700	-46.5	2
>CHCl	CH ₂ COO	3	23	22	2.14	-0.90	4

^a >CH₂ class includes CH₃ and >CH; =CH (arom) class includes =C < (arom); CH₂COO class includes >CHCOO and -CCOO.

Table IV
Equation of State Information Used in Calculations for the PMMA/PVC System

names of polymer components (up to four characters long)		PMMA	PVC
molecular weight of repeat unit	M_u	100.1	62.5
weight-average molecular weight	M_w	60 000	55 000
coefficients of specific volume vs temperature polynomial	a	0.8254	0.7183
$v = a + bt + ct^2 + dt^3$	b	2.838×10^{-4}	2.924×10^{-4}
(t in °C, v in cm ³ /g)	c	7.792×10^{-7}	9.747×10^{-7}
coefficients of the Tait	d	0	0
parameter $B_{Tait} = B_0$	B_0	2875.0	2989.0
$\exp(-B_1t)$ (t in °C, B in bar)	B_1	4.15×10^{-3}	3.86×10^{-3}
characteristic equation of state	v^*	0.8035	0.6890
parameters (v^* in cm ³ /g, T^* in K, P^* in cal/cm ³)	T^*	757.0	675.0
	P^*	123.7	182.5

expansion and compressibility information over the temperature range 100–200 °C by application of eqs 22–24. The parameters are substantially the same as those reported elsewhere³⁶ for this system, thus indicating the accuracy of our procedures.

The structural groups used in the MGQ calculation are summarized in Table II. The identification of groups follows that recommended by Bondi,³⁷ as does the calculation of the surface area parameter, q_i . The choice of classes of groups follows Lai et al.^{22,23} and Abrams and Prausnitz.¹⁹ For example, the CH₂ class also includes CH₃ and >CH groups, because these groups are found to function identically in correlating the data. Similarly, the aromatic carbon class, Tables II and III, include =C< and =CH groups.

Table III gives the values of the group interaction energy, ΔE_{ij} , and entropy, A_{ij} , parameters required by the MGQ model for the three binary systems presented in this paper. Values of the interaction parameters describing the interaction of the methoxy functional group were determined for this work from literature heats of mixing data^{41,42} and previously determined interaction parameters for the other functional groups in the data set.^{22–24} The percent root-mean-square (% rms) error associated with methoxy group interactions with alkane and aromatic carbon functional groups were 3% and 6% for 27 and 13 data points, respectively. These results indicate that a quite acceptable fit of the data to the model is obtained when the interaction parameters in Table III are used to describe the heats of mixing of the experimental liquids.

PMMA/PVC. Table IV shows the input parameters used in calculating the equation of state contributions to the spinodal. The specified molecular weights are those specified by Jager et al.³¹ in their study of phase splitting on heating through observation of optical cloud points. Their cloud point data are used for comparison with the calculated spinodal, below. The volume dilatation parameters for poly(methyl methacrylate) (PMMA) are

Table V
Structural Group Assignments and Characteristics for the PMMA/PVC System

structural group	MW/ <i>q</i>	type no.	class no.	no. of groups in PMMA	no. of groups in PVC
CH ₃	15.04/0.848	1	1	2	0
>CH ₂	14.03/0.540	2	1	1	1
>CC(O)O	56.02/0.888	3	2	1	0
>CHCl	48.47/0.952	4	3	0	1

Table VI
Equation of State Information Used in Calculations for the PMMA/PEO System

names of polymer components (up to four characters long)		PMMA	PEO
molecular weight of repeat unit	M_u	100.1	44.0
weight-average molecular weight	M_w	130 000	300 000
coefficients of specific volume vs temperature polynomial	a	0.8254	0.8777
$v = a + bt + ct^2 + dt^3$	b	2.838×10^{-4}	6.107×10^{-4}
(t in °C, v in cm ³ /g)	c	7.792×10^{-7}	2.620×10^{-7}
coefficients of the Tait	d	0	0
parameter $B_{Tait} = B_0$	B_0	2875.0	2121.3
$\exp(-B_1t)$ (t in °C, B in bar)	B_1	4.15×10^{-3}	3.99×10^{-3}
characteristic equation of state	v^*	0.8035	0.8611
parameters (v^* in cm ³ /g, T^* in K, P^* in cal/cm ³)	T^*	757.0	687.0
	P^*	123.7	121.0

obtained by curve fitting the PVT data obtained by Olabisi and Simha,⁴³ while those for PVC were obtained by fitting the equation of state given by Beret and Prausnitz.⁴⁴ These parameters were obtained for temperatures between 100 and 200 °C.

The structural groups in the repeat structures of PMMA and PVC and their Bondi³⁷ area parameters system are shown in Table V. The interaction parameters corresponding to the interaction of these groups is shown in Table III. As discussed in Lai et al.,²² the researchers obtained the interaction parameters for the CH₂/CHCl and for the CHCl/CH₂COO interacting pairs by simultaneous regression, as opposed to their usual practice or regressing on one set of unknown ΔE_{ij} and A_{ij} parameters at a time. This approach was found to better fit the heats of mixing data measured by the authors.

PMMA/PEO. Table VI shows the input parameters used for calculating equation of state parameters. The molecular weights reported here are those reported by Fernandes in her study of the cloud points of PMMA/poly(ethylene oxide) (PEO) mixtures.^{30,45} These data are used for experimental comparisons with the model, below. The Tait and polynomial parameters for PMMA are taken to be the same as those reported in Table IV. The parameters for PEO were obtained by curve fitting PVT data for PEO given by Jain and Simha.⁴⁶ These parameters were used to calculate the characteristic parameters for PEO over the temperature range 100–200 °C.

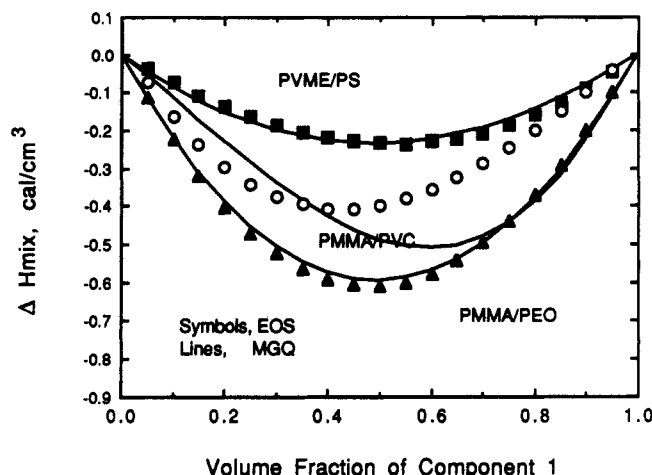


Figure 2. Comparison of heats of mixing at the spinodal. —, estimates from MGQ; ■, estimate from SLB for PVME/PS; ○, estimate from SLB for PMMA/PVC; ▲, estimate from SLB for PMMA/PEO.

Table VII
Structural Group Assignments and Characteristics for the PMMA/PEO System

structural group	MW/q	type no.	class no.	no. of groups in PMMA	no. of groups in PEO
CH ₃	15.04/0.848	1	1	2	0
>CH ₂	14.03/0.540	2	1	1	1
>CC(O)O	56.02/0.888	3	2	1	0
CH ₂ O	30.03/0.780	4	3	0	1

Table VIII
Summary of Estimated Parameters

system	ϵ_{12}^*/k , K	$\delta\epsilon^*/k$, K	SE in ΔH_{mix} estimate, %
PS/PVME	652.6 ± 1.5	447.4 ± 16.7	8.8
PMMA/PEO	646.8 ± 0.7	740.9 ± 7.9	3.9
PMMA/PVC	672.0 ± 7.5	451.5 ± 84.4	37.7

The structural groups and their Bondi area parameters are shown in Table VII. These groups are used with the MGQ interaction parameters in Table III to estimate the heat of mixing at the spinodal, as described above.

Results and Discussion

Figure 2 summarizes a comparison between the MGQ heat of mixing evaluated at the spinodal temperature and composition, eq 12, with that computed from eq 35 by using the "best fit" parameters, ϵ_{12}^* and $\delta\epsilon^*$, summarized in Table VIII. Generally, the calculated heats of mixing are small and negative at the spinodal, as expected from the SLB model. Quite good agreement between the heats of mixing estimated by the SLB and MGQ models is seen for both PMMA/PEO and PVME/PS binaries. The errors between the SLB heats of mixing relative to the MGQ model estimates are only 4% and 9%, for PMMA/PEO and PVME/PS, respectively, and both models show substantially the same variation of heat of mixing with composition at the spinodal. On the other hand, the agreement between the heats of mixing of the two models is quite poor for the PMMA/PVC binary, as evidenced by a 38% relative error. The reason for this behavior seems to be related to the different curve shapes predicted by the models for this system. The computer fitting technique appears to be attempting to minimize error; however, the SLB model cannot skew sufficiently with composition to fit the minimum required by the MGQ model.

Figure 3 shows a comparison of the heats of mixing for

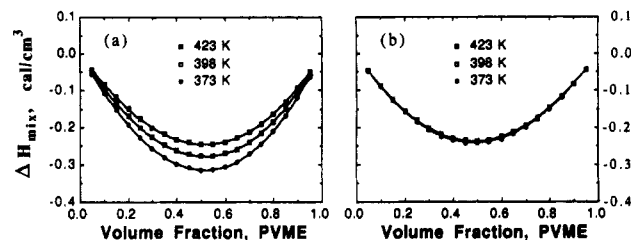


Figure 3. Comparison of heats of mixing estimates for the PVME/PS system at various isothermal temperatures. (a) estimated from SLB model; (b) estimated from MGQ model.

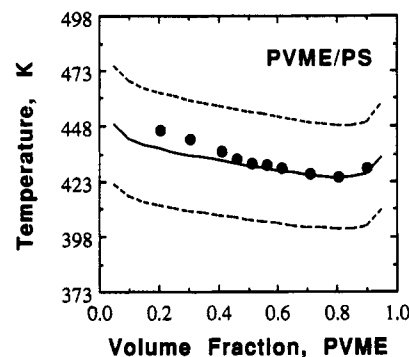


Figure 4. Spinodal diagram for the PVME/PS binary. —, calculated; - - -, calculated error limits; ●, experimental.

the PVME/PS system as calculated at several isothermal temperatures by the MGQ and SLB models. The best fit parameters to the MGQ model at the LCST, Table VIII, are used for this comparison. Although the excess heat capacity, $C_p^E = d\Delta H_{\text{mix}}/dT$, predicted by the SLB model is small, roughly +0.0015 cal/(cm³ °C), it predicts a larger, positive, C_p^E than that predicted by the MGQ model. Interestingly, the C_p^E value predicted by the SLB model is itself nearly a factor of 10 lower than measured C_p^E values³⁴ in miscible blends other than PVME/PS. Since it is doubtful that excess heat capacities vary by a factor of 10 as the polymeric constituents in the miscible binary are changed, one could conclude that neither model is able to correctly predict the temperature dependency of the heat of mixing. The equation of state contributions in the SLB model, alone, are apparently insufficient to explain the excess heat capacity. Likewise, the nearly zero C_p^E predicted by the MGQ model results from the low ΔE_{ij} interaction energies associated with the structural groups in the PVME and PS repeat structures in this model.

Figure 4 compares the predicted PVME/PS spinodal with the experimental data of Han et al.²⁹ These data are obtained from small-angle neutron scattering experiments and are thought to accurately represent the spinodal transition. Very good agreement is seen between the experimental and predicted spinodal, using the calculational procedures outline above. The dashed lines in Figure 4 represent the boundaries of uncertainty associated with the prediction. These uncertainties include the uncertainties reported in Table VIII, which are related to inconsistencies between the MGQ and SLB models as well as to uncertainties in experimental values required for the computation. As indicated in Figure 4, these uncertainties cause the spinodal temperature to be uncertain by approximately 25 K.

Figure 5 compares the predicted spinodal for PMMA/PVC with the cloud points reported by Jager et al.³¹ Despite quite different predictions by the two models for ΔH_{mix} at the spinodal, Figure 2, which lead to estimated uncertainties as high as ±100 K in the location of the

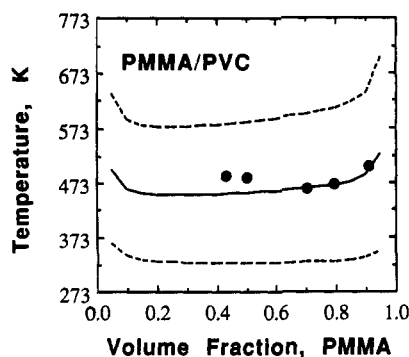


Figure 5. Spinodal diagram for the PMMA/PVC binary. —, calculated; ---, calculated error limits; ●, experimental cloud points.

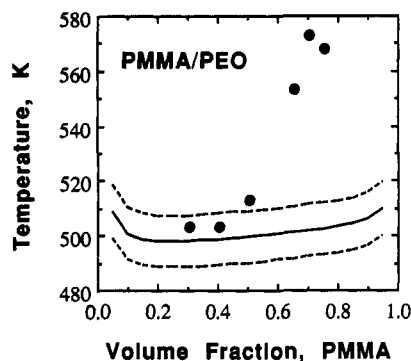


Figure 6. Spinodal diagram for the PMMA/PEO binary. —, calculated; ---, calculated error limits; ●, experimental cloud points.

spinodal temperature, the differences between experimental cloud points and calculated spinodal are less than 20 K. Interestingly, the calculated spinodal appears to fit the experimental data somewhat better in the PMMA-rich regime, where the heats of mixing, calculated by the MGQ model, are better fit to the SLB model (see Figure 2).

Figure 6 shows the comparison between the experimental cloud point data of Fernandes^{30,45} and the calculated spinodal for the PMMA/PEO system. Despite quite good agreement between the two models, as implied by the low uncertainty in energetic parameters, Table VIII, and the correspondingly small error bounds, Figure 6, the agreement between experiment and calculation is rather poor. The reason for the poor prediction in this case has not been identified. One possibility for the discrepancy may be slow kinetics of phase growth to the size necessary to scatter white light. The experimental measurements were made with optical light by placing the sample in a cavity that was heated at between 5 and 10 °C/min, following a procedure described previously.²⁵ If the kinetics of phase growth were slow, the detected transition could occur at temperatures that are greater than the actual spinodal. This problem may always be of some concern when one attempts to compare the temperature at which spinodal decomposition occurs with that associated with an optically determined cloud point. The good agreement shown in Figures 4 and 5 between experimental cloud points and spinodal prediction may therefore be a fortunate consequence of phase-growth kinetics and optical properties in those particular systems.

Summary and Conclusions

The procedure outlined in this paper for predicting the spinodal in miscible polymer blends is an engineering approach that combines the MGQ group contribution

model for estimating the heat of mixing at the spinodal with the SLB generalized lattice fluid equation of state model. Neither model could be used separately to estimate the temperature location of the spinodal. The MGQ model estimates only ΔH_{mix} and its derivatives with temperature and composition. No mechanism is provided in this model for spinodal decomposition. The SLB model provides the needed mechanism; however, there is no independent way to determine the energy parameters, ϵ_{12}^* and $\delta\epsilon_{12}^*$, needed for estimating the spinodal.

The two models are not conceptually consistent with one another, as indicated by their quite different estimates of excess heat capacity. Despite this inconsistency, the ΔH_{mix} estimates obtained from the MGQ model at temperatures near the spinodal are close enough to reality to permit good estimates of the spinodal decomposition temperature to be made when the ΔH_{mix} estimates are used to estimate the energy parameters in the SLB model.

Comparison of the LCSTs, Figures 4–6, for the three systems studied with the corresponding magnitudes of their exothermic heats of mixing at their spinodals, Figure 2, is qualitatively consistent with previous experimental observations;¹⁵ the more exothermic the heat of mixing, the higher the temperature at which phase separation occurs. If one plots the phase separation temperature at $\Phi_1 = 0.5$ vs the absolute value of the heat of mixing at that composition, the slope of the approximate line that results is ~ 200 °C/(cal/mL) for the systems studied here. This compares fairly well to a slope of approximately 400 °C/(cal/mL) for poly(vinylidene fluoride) (PVF₂) containing systems where ΔH_{mix} is determined experimentally from melting point depression of the PVF₂ in blends with polyesters.¹⁵ The difference between these observations, a factor of 2, could be a consequence of differences in the two systems, caused by the presence of weak hydrogen bonding in the PVF₂-containing blends. The difference could just as well be a consequence of measurement and extrapolation errors. In still other systems where the comparison can be made,^{23,24} similar differences in the heats of mixing are observed; however, in these cases the ΔH_{mix} obtained from liquid heats by the MGQ model is a factor of 2 lower than that observed from melting point depressions.

Given the extreme sensitivity of the temperature location of the spinodal to the magnitude of the exothermic heat of mixing, the thermal extrapolations and other approximations and assumptions associated with estimating ΔH_{mix} at the spinodal with the MGQ model, and the similar uncertainties in experimental data and approximations associated with the SLB model, it is quite amazing that the predictive scheme works as well as it does. The success of the combined models suggests that one ought to be able to write a nonrandom lattice fluid theory that successfully integrates the major concepts of both the MGQ and SLB models. Until that is accomplished, the procedure discussed here can be employed to give hopefully reasonable estimates of the spinodal boundary in miscible polymer blends.

Acknowledgment. The partial support for portions of this work by the National Science Foundation, through Research Grant DMR-86-03131, is gratefully acknowledged. We also acknowledge the technical advice provided by Dr. I. C. Sanchez of this department.

Glossary

A_{ij}	MGQ parameter related to exchange entropy, ΔS_{ij}
A_{wi}	Bondi area for structural group i in MGQ theory (cm ² /mol)

$B(T)$	Tait parameter used for estimating compressibility (bar)
B_0	coefficient in Tait equation (bar)
B_1	coefficient in Tait equation (K^{-1})
B_{ij}	MGQ interaction energy density for mixture (cal/cm^3)
$B_{ij}^{(k)}$	MGQ interaction energy density for groups i and j in pure component k (cal/cm^3)
D	mathematical term in SLB model
d	number of ways ($d = 10$ assigned) specific 1-2 interaction can occur in the SLB model
ΔE_{ij}	MGQ exchange energy of formation of i - j pair (cal/mol)
f	number of structural groups in the system defined by the MGQ model
G	free energy of a binary system in the SLB model (cal)
ΔG_{mix}	free energy of mixing (cal)
g	free energy per mer units in SLB model (cal)
g_{12}^*	free energy per mer associated with specific interaction in the SLB model (cal)
ΔH_{mix}	enthalpy of mixing of pure components (cal)
$\Delta H_{\text{mix}}'$	enthalpy of mixing per unit volume (cal/cm^3)
h	enthalpy of mixture per mer in SLB model (cal)
K_{ij}	apparent equilibrium constant in the MGQ model, which describes the fraction of i - j pairs in the system
k	Boltzmann constant (cal/K)
N_i	number of molecules of type i in SLB model (mol)
n_i	number of groups of type i in MGQ model (mol)
N_{ij}	number of i - j contacts in MGQ model (mol)
P_i^*	characteristic pressure for pure component i in the SLB model (cal/cm^3)
P_r	reduced pressure, P/P_i^* , in the SLB model
q_i	surface area parameter of group i in MGQ model (cm^2/mol)
R	ideal gas law constant ($\text{cal}/(\text{mol K})$)
r_i	number of lattice sites in SLB model occupied by component i
ΔS_{ij}	exchange entropy for formation of i - j pair in MGQ model ($\text{cal}/(\text{mol K})$)
ΔS_{mix}	entropy of mixing (cal/K)
s_c	combinatorial entropy per mer in SLB model for mixing occupied sites (cal/K)
s_v	combinatorial entropy per mer in SLB model for mixing vacant and occupied sites (cal/K)
T	absolute temperature (K)
T_i^*	characteristic temperature in SLB model (K)
T_r	reduced temperature, T_i/T_i^* , in SLB model
ΔU_{mix}	potential energy of mixing of pure components in MGQ model (cal)
V	system volume (cm^3)
v	specific volume (cm^3/g)
z	coordination number in MGQ model
β_{i0}	pure component compressibility (bar^{-1})
$\Delta \epsilon^*$	exchange energy per mer in the SLB model (cal)
$\delta \epsilon^*$	energy parameter per mer in the SLB model that is associated specific interactions (cal)
ϵ_i^*	characteristic energy of interaction for component i in the SLB model (cal)
ϵ_T^*	characteristic energy for mixture in SLB model (cal)
ϵ_{12}^*	energy parameter per mer that is associated with nonspecific interactions (cal)
ν_{oi}	characteristic volume per mole of sites for pure component i in the SLB model (cm^3/mol)
ν_o	characteristic volume per mole of sites in SLB model (cm^3/mol)

ρ_i	density of pure component i (g/cm^3)
ρ_i^*	characteristic density of pure component i (g/cm^3)
ρ_r	reduced density, ρ/ρ^* , in SLB model
Γ_{ij}	nonrandom parameter in MGQ model
Ψ_i	area fraction of group i in MGQ mixture
$\Psi_i^{(k)}$	area fraction of group i in pure component k in MGQ model
Φ_i	volume fraction of component i
Ω	term in SLB model

References and Notes

- (1) Olabisi, O.; Robeson, L. M.; Shaw, M. T. *Polymer-Polymer Miscibility*; Academic Press: New York, 1979.
- (2) Paul, D. R.; Newman, S., Eds. *Polymer Blends*; Academic Press: New York, 1978; Vols. I, II.
- (3) Paul, D. R.; Barlow, J. W. *J. Macromol. Sci., Rev. Macromol. Chem.* 1980, 18, 109.
- (4) Barlow, J. W.; Paul, D. R. *Annu. Rev. Mater. Sci.* 1981, 11, 299.
- (5) Flory, P. J. *Principles of Polymer Chemistry*; Cornell University Press: Ithaca, NY, 1953.
- (6) Walsh, D. J.; Higgins, J. S.; Maconnachie, A., Eds. *Polymer Blends and Mixtures*; NATO Series E 89; Martinus Nijhoff Publishers: Dordrecht, The Netherlands, 1985.
- (7) Christiansen, W. H.; Paul, D. R.; Barlow, J. W. *J. Appl. Polym. Sci.* 1987, 34, 537.
- (8) Barlow, J. W.; Paul, D. R. *Polym. Eng. Sci.* 1987, 27, 1482.
- (9) Woo, E. M.; Barlow, J. W.; Paul, D. R. *J. Appl. Polym. Sci.* 1986, 36, 3889.
- (10) Pfennig, J. L.; Keskkula, H.; Barlow, J. W.; Paul, D. R. *Macromolecules* 1985, 18, 1937.
- (11) Paul, D. R.; Barlow, J. W. *Polymer* 1984, 25, 487.
- (12) Harris, J. E.; Paul, D. R.; Barlow, J. W. *Polym. Eng. Sci.* 1983, 23, 676.
- (13) Ziska, J. J.; Barlow, J. W.; Paul, D. R. *Polymer* 1981, 22, 918.
- (14) Cruz, C. A.; Barlow, J. W.; Paul, D. R. *Macromolecules* 1979, 12, 726.
- (15) Paul, D. R.; Barlow, J. W.; Bernstein, R. E.; Wahrmond, D. C. *Polym. Eng. Sci.* 1978, 18, 1225.
- (16) Guggenheim, E. A. *Proc. R. Soc. London* 1944, A183, 213.
- (17) Staverman, A. J. *Recl. Trav. Chim. Pays-Bas* 1937, 56, 885, 1189.
- (18) Bondi, A. J. *Phys. Chem.* 1964, 68, 441.
- (19) Abrams, D. S.; Prausnitz, J. M. *AIChE J.* 1975, 21, 116.
- (20) Rowlinson, J. S. *Liquids and Liquid Mixtures*; Academic Press: New York, 1967.
- (21) Panayiotou, C.; Vera, J. H. *Fluid Phase Equilib.* 1980, 5, 55.
- (22) Lai, C. H.; Paul, D. R.; Barlow, J. W. *Macromolecules* 1988, 21, 2492.
- (23) Lai, C. H.; Paul, D. R.; Barlow, J. W. *Macromolecules* 1989, 22, 374.
- (24) Barlow, J. W.; Lai, C. H.; Paul, D. R. Prediction of Polymer-Polymer Miscibility with a Group Contribution Method. In *Contemporary Topics in Polymer Science*; Culbertson, B. M., Ed.; Plenum Press: New York, 1989; Vol. 6, pp 505-517.
- (25) Bernstein, R. E.; Cruz, C. A.; Paul, D. R.; Barlow, J. W. *Macromolecules* 1977, 10, 681.
- (26) Nolley, E.; Barlow, J. W.; Paul, D. R. *J. Appl. Polym. Sci.* 1979, 23, 632.
- (27) McMaster, L. P. *Adv. Chem. Ser.* 1975, No. 142, 43.
- (28) McMaster, L. P. *Macromolecules* 1973, 6, 760.
- (29) Han, C. C.; Baurer, B. J.; Clark, J. C.; Muroga, Y.; Matsushita, Y.; Okada, M.; Tran-Cong, Q.; Chang, T.; Sanchez, I. *Polymer* 1988, 29, 2002.
- (30) Fernandes, A. C.; Barlow, J. W.; Paul, D. R. *J. Appl. Polym. Sci.* 1986, 32, 5481.
- (31) Jager, H.; Vorenkamp, E. J.; Challa, G. *Polym. Commun.* 1983, 24, 290.
- (32) Pearce, E. M.; Kwei, T. K.; Min, B. Y. *J. Macromol. Sci., Chem.* 1984, 21, 1181.
- (33) ten Brinke, G.; Karasz, F. E. *Macromolecules* 1984, 17, 815.
- (34) Barnum, R. S.; Goh, S. H.; Barlow, J. W.; Paul, D. R. *J. Polym. Sci., Polym. Lett. Ed.* 1985, 23, 395.
- (35) Sanchez, I. C.; LaCombe, R. H. *Macromolecules* 1978, 11, 1145.
- (36) Sanchez, I. C.; Balazs, A. C. *Macromolecules* 1989, 22, 2325.
- (37) Bondi, A. *Physical Properties of Molecular Crystals, Liquids and Gases*; Wiley: New York, 1968.
- (38) Richardson, M. J.; Saville, N. G. *Polymer* 1977, 18, 3.
- (39) Uriarte, C.; Eguiázabal, J. I.; Llanos, M.; Iribarren, J. I.; Iruin, J. J. *Macromolecules* 1987, 20, 3038.
- (40) Simha, R.; Wilson, P. S.; Olabisi, O. *Kolloid Z. Z. Polym.* 1973, 251, 402.

- (41) Sosnkowska-Kehiaian, K.; Hryniewicz, R.; Kehiaian, H. *Bull. Acad. Pol. Sci., Ser. Sci. Chim.* **1969**, *17*, 1969.
- (42) Kehiaian, H. V.; Sosnkowska-Kehiaian, K.; Hryniewicz, R. *J. Chim. Phys. Phys.-Chim. Biol.* **1971**, *68*, 922.
- (43) Olabisi, O.; Simha, R. *Macromolecules* **1975**, *8*, 206.
- (44) Beret, S.; Prausnitz, J. M. *Macromolecules* **1975**, *8*, 878.
- (45) Fernandes, A. C. Ph.D. Dissertation, The University of Texas at Austin, 1986.
- (46) Jain, R. K.; Simha, R. *J. Polym. Sci., Polym. Phys. Ed.* **1979**, *17*, 1929.
- (47) Elliot, K.; Wormald, C. J. *J. Chem. Thermodyn.* **1976**, *8*, 881.
- (48) Diaz-Pena, M.; Menduina, C. *J. Chem. Thermodyn.* **1974**, *6*, 387.
- (49) Munch, E. *Thermochim. Acta* **1978**, *22*, 237.
- (50) Romani, L.; Paz-Andrade, M. I. *An. Quim.* **1974**, *70*, 422.
- (51) Grolier, J.-P. E.; Ballet, D.; Viallard, A. *J. Chem. Thermodyn.* **1974**, *6*, 895.
- (52) Otin, S.; Thomas, G.; Peiro, J. M.; Velasco, I.; Gutierrez-Losa, C. *J. Chem. Thermodyn.* **1980**, *12*, 955.
- (53) Dusart, O.; Piekarski, S.; Grolier, J.-P. E. *J. Chim. Phys. Phys.-Chim. Biol.* **1979**, *76*, 433.
- (54) Delmas, G.; Thank, N. T. *J. Chem. Soc., Faraday Trans. 1* **1975**, 1172.
- (55) Hirobe, H. *J. Fac. Sci., Imp. Univ. Tokyo* **1926**, *1*, 155.

Registry No. PVME, 9003-09-2; PS, 9003-53-6; PMMA, 9011-14-7; PVC, 9002-86-2; PEO, 25322-68-3.